THE JOURNAL OF PHYSICAL CHEMISTRY B

Article

pubs.acs.org/JPCB

Photoelectron Spectra of Some Important Biological Molecules: Symmetry-Adapted-Cluster Configuration Interaction Study

Hossein Farrokhpour* and Maryam Ghandehari

Chemistry Department, Isfahan University of Technology, Isfahan, 84156-83111, Iran

Supporting Information

ABSTRACT: In this work, the valence vertical ionization energies (up to 5) of some important biologically active molecules including 2,4-dinitrophenol, 2,4-dinitroanisole, nicotinic acid, nicotinic acid methyl ester, nicotinamide, *N*,*N*-diethylnicotinamide, barbituric acid, uric acid, cytosine, β-carotene, and menadione were calculated in the gas phase and compared with the experimental data reported in the literature. The symmetry-adapted-cluster configuration interaction (SAC-CI) general-R method was used to calculate the ionization energies. The intensity of each ionization band was evaluated using the monopole approximation. Comparison of the calculated photoelectron spectrum of each molecule with its corresponding experimental spectra allowed for assigning the photoelectron bands by natural bonding orbital (NBO) calculations even though some of the associated bands were significantly overlapped for some molecules. Among the considered molecules, there was no agreement between the experimental and calculated photoelectron spectrum of β-carotene. The reason for this disagreement was theoretically investigated and attributed to the degradation and decomposition of β-carotene. The calculated first ionization energies of the considered molecules were correlated with their Hückel *k*-index to obtain Coulomb (α) and resonance (β) integrals of the Hückel molecular orbital theory for the biomolecules considered in this study. A linear correlation was found between the first ionization energy and the Hückel *k*-index.

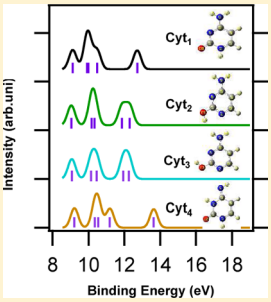

1. INTRODUCTION

Photoelectron spectroscopy is a powerful technique that is mostly used for determining ionization energies of atoms and molecules. The atom or molecule can be ionized from valence or core orbital depending on the radiation energy. The main goal in photoelectron spectroscopy is to gain information about composition, electronic state, chemical state, and binding energy.[1] The photoelectron spectrum of each atom or molecule provides valuable information on its electronic structure. Electronic structure calculations are necessary to understand and identify the electronic states involved in the photoelectron spectrum of each molecule.[1]

Gas-phase experimental and theoretical information on the fundamental properties of biological molecules are very important in understanding many biological phenomena and providing insight into the physicochemical origin of the properties of biological molecules.[2−5] One of the most important physicochemical properties of biomolecules is their ionization potentials which are useful quantum mechanical diagnostics for oxidative potentials of these molecules. For example, when a photoionization or photoabsorption process occurs in a biological system such as living cells, it may cause certain photobiological effects on the system such as damage, cell death, or mutation. Therefore, knowing the values of ionization energies of biomolecules is important for unraveling the mechanism of protein, DNA, and cell damage due to photoionization.

Valence ionization of biologically active compounds gives information about the frontier orbitals which significantly change in the species and chemical reactions. In this regard, there are numerous gas-phase He-I and He-II photoelectron spectra of different biological molecules in the literature.[6−14] Recently, photoelectron spectroscopy with the aid of high level of computational chemistry has significantly contributed to the determination of the vertical ionization energies and elucidation of the structure and dynamic of biomolecules and their solvated complexes in the gas phase.[15−26] For example, photoelectron spectroscopy along with the ab initio calculations was employed to determine the population ratios of different conformers and tautomers of amino acids and nucleotides in the gas phase.[17] In another example, effect of solvation on the vertical ionization energies of amino acids and nucleotides in microhydration and bulk conditions has been also investigated both experimentally and theoretically.[15,16]

There are two limitations for directly extracting ionization energies from the observed features in the recorded photoelectron spectra, especially for biological molecules. The first limitation is related to the overlap of the ionization bands so that the spectrum exhibits broad overlapping bands with little evidence of vibrational structure. Therefore, the assignment of spectrum based only upon the ionization energies obtained for the observed features is complicated and ambiguous because, in many cases, ionizations from more than one orbital are combined to form a single band. The second limitation is related to the molecules with more than one stable conformers and tautomers. In this case, the recorded photoelectron

Received: November 13, 2012
Revised: April 20, 2013

   dx.doi.org/10.1021/jp311213c | *J. Phys. Chem. B* XXXX, XXX, XXX−XXX

spectrum is related to more than one conformer and tautomer and it is a weighted sum of the photoelectron spectra of the contributing tautomers and conformers. Considering these two limitations, it is difficult to obtain information from photoelectron spectrum without any theoretical calculations. These two limitations are more evident in the assignment and interpretation of the photoelectron spectra of biomolecules. To remove these limitations, high-level ab initio calculations are necessary for describing and assigning the photoelectron spectra and revealing subtle differences caused by various chemical environments, conformations, and tautomers.

One of the most important cautions which should be considered in the gas-phase photoelectron spectroscopy of biological molecules is checking the stability of the sample upon heating. Some of the biological molecules (especially, large ones) decompose before reaching the gas phase. This is the most challenging part of the photoelectron spectroscopy of biological molecules in the gas phase; thus, using a temperature at which decomposition occurs should be avoided. The species resulting from decomposition of the sample add new ionization bands to the spectrum and lead to changes in the relative intensity of peaks in the main spectrum. Most of the He-I and He-II photoelectron spectra of biological molecules were recorded in the late 1970s and early 1980s without checking the degradation of the sample due to heating. Some of the spectra have been recorded at high temperatures (300 −350 °C) to reach suitable pressure for recording the spectra. In this case, the ab initio calculation of photoelectron spectrum can be used as one of the guides for checking the accuracy of the recorded spectrum.

In this work, the photoelectron spectra of some important biological compounds including 2,4-dinitrophenol (DNP), 2,4-dinitroanisole (DNAN), nicotinic acid (NA), nicotinic acid methyl ester (NAME), nicotinamide (NAM), *N*,*N*-diethylnicotinamide (DNAM), barbituric acid (BA), cytosine (Cyt), uric acid, β-carotene, and menadione were calculated and compared with their recorded photoelectron spectra reported by Dougherty et al.[6] This allowed for assigning the photoelectron bands by natural bonding orbital (NBO) calculations even though some of the associated bands were significantly overlapped for some molecules. To the best of the authors' knowledge, there are no ab initio calculations on ionization energies and assignment of the photoelectron spectra of the considered biomolecules in the literature, except cytosine. In addition, effects of the substituents on the values of ionization energies as well as the influence of different tautomers and conformers on the photoelectron spectra of some molecules were investigated. Finally, the first ionization potential of these molecules were correlated with their Hückel *k*-index to obtain accurate values for the Coulomb (α) and resonance (β) integrals in the Hückel molecular orbital theory.

2. COMPUTATIONS

Geometries of the conformers and tautomers of each molecule were optimized at the B3LYP/aug-cc-pVDZ level of theory. The Gibbs free energies of the conformers and tautomers of each molecule were calculated at the B3LYP/aug-cc-pVDZ level of theory to obtain their Boltzmann population ratios. To calculate the photoelectron spectrum of each molecule, the Boltzmann population ratios of its conformers and tautomers are necessary. Each optimized structure was separately used to calculate the energies of its vertical outer valence photoelectron spectrum using a very accurate computational method such as SAC-CI general-R method[27−30] and the 6-31+G(d) basis set. The SAC-CI method has been successfully applied to several molecular spectroscopic problems including ionization spectroscopy.[31−37] Generally, there are two standard SAC-CI methods with respect to the choice of excitation operators. In the SAC-CI SD (single double)-R method, single and double excitation operators are used while the SAC-CI general-R method further involved triple and higher excitation operators (up to six). The SAC-CI general-R method can describe multiple-electron processes with high accuracy. This method has been shown to be efficient for studying a large number of states in the ionization spectrum.[38,39]

Single excitation operators were included without selection and the double excitation operators were included when its second-order contribution in energy was larger than a given threshold ($\lambda = 10^{-6}$; level three) in the SAC calculations to obtain energy and wave function of the ground state of the neutral molecule. For unlinked operators, the products of linked operators whose SDCI coefficients of higher than 5×10^{-3} were also used in SAC calculations. The active space consisted of all occupied orbitals and unoccupied orbitals: only 1s orbitals were frozen as core orbitals and the calculated SAC wave function was used for the general-R calculations. In the general-R method, exponential generation algorithm was used to produce a higher order linked operator (more than triple). Single excitation operator was used without selection and the double excitation operators were handled as in the SAC-CI SD-R method. Triple and quadruple excitation operators were produced as products of single and double excitation operators, the coefficients of which were higher than 0.04 in the SAC-CI SD-R calculation. Quintuple and sextuple excitation operators were generated by the product of one and two double excitation operators and the product of three double excitation operators, respectively. In the present calculations, the excitation operators, up to sextuple excitations (MaxR = 6), were included in the general-R calculations. The prepared Gaussian input file of one of the considered molecules (nicotinamide) was reported in the Supporting Information. For more information on the SAC-CI method, the readers can refer to the SAC-CI home page.[40]

The ionization cross sections were calculated using the monopole approximation,[41] which allowed for the correct estimation of relative intensity of the peaks. In calculating the monopole intensities, the correlated SAC wave function of the ground electronic state of neutral molecule and SAC-CI general-R wave functions of ionic electronic states were used. Furthermore, NBO calculations using Gaussian NBO (version 3.1)[42] were performed at the Hartree−Fock (HF)/6-31+G(d) level of theory to calculate the molecular orbitals at the ground electronic state for the spectral band assignment. Since the calculation at the SAC-CI general-R is time consuming, a moderate basis set such as 6-31+G(d) was used for the calculations. But, it should be noticed that the selected basis set has enough polarization and diffuse functions for describing the outer valence ionization band of the considered molecules. All of the calculations were performed using Gaussian 09 quantum chemistry package.[43]

To evaluate the reliability of the proposed computational method for calculating the ionization energies, the seven ionization energies of aniline molecule were calculated because its experimental ionization energies have been reported in the literature and it has similarity with the most of the biological molecules selected in this work. Aniline has an aromatic ring

dx.doi.org/10.1021/jp311213c | J. Phys. Chem. B XXXX, XXX, XXX−XXX

Table 1. Comparison of Vertical Ionization Energies (I), Calculated at the SAC-CI General-R/6-31+G(d) Level of Theory with the Corresponding Experimental Values for the Selected Molecules in This Work[a]

compound	I_1 (eV)	I_2	I_3	I_4	I_5
DNP	9.692 (0.775)	10.769 (0.773)	11.373 (0.728)	11.515 (0.736)	11.912 (0.730)
	9.85[b]	10.70[b]	11.40[b]	11.70[b]	11.70[b]
DNAN	9.177 (0.793)	10.171 (0.792)	10.909 (0.748)	10.997 (0.759)	11.173 (0.760)
	9.55[b]	10.400[b]	11.100[b]	11.400[b]	11.400[b]
NA	NA_1 9.389 (0.916)	10.419 (0.918)	12.930 (0.935)	13.705 (0.922)	13.982 (0.924)
	NA_2 9.357 (0.919)	9.459 (0.948)	10.166 (0.942)	10.228 (0.918)	11.632 (0.925)
	9.61[c]	10.000[b]	10.77[b]	10.930[b]	11.900[b]
NAME	9.530 (0.801)	9.710 (0.772)	10.267 (0.795)	10.633 (0.770)	11.321 (0.783)
	9.99[d]	9.850[b]	?	10.650[b]	11.250[b]
NAM	NAM_1 9.414 (0.809)	9.507 (0.804)	9.975 (0.806)	10.265 (0.810)	13.106 (0.773)
	NAM_2 9.237 (0.810)	9.480 (0.805)	10.050 (0.808)	10.171 (0.802)	13.144 (0.756)
	9.13[b]	9.850[b]	?[b]	10.350[b]	10.750[b]
DNAM	$DNAM_1$ 7.946 (0.814)	8.299 (0.812)	8.854 (0.822)	9.310 (0.813)	9.676 (0.822)
	$DNAM_2$ 8.020 (0.813)	8.336 (0.810)	8.981 (0.813)	9.359 (0.808)	9.668 (0.817)
	8.530[b]	9.0[b]	9.4 ± 0.2[b]	9.98[b]	10.54[b]
UA	8.092 (0.962)	10.260 (0.908)	10.752 (0.935)	10.778 (0.922)	11.324 (0.943)
	8.550[b]	10.500[b]	10.700[b]	11.200[b]	11.80[b]
Cyt	Cyt_1 8.570(0.799)	9.373 (0.799)	9.438 (0.771)	9.927 (0.777)	12.170 (0.778)
	8.17[e]	8.93[e]	9.46[e]	9.91[e]	11.90[e]
	8.63[f]	9.37[f]	9.85[f]	10.41[f]	12.22[f]
	8.79[g]	9.54[g]	9.64[g]	9.96[g]	12.08[g]
	Cyt_2 8.488 (0.810)	9.626 (0.802)	9.779 (0.807)	11.322 (0.7917)	11.751 (0.793)
	8.40[e]	9.49[e]	9.65[e]	11.25[e]	11.66[e]
	8.64[f]	9.69[f]	9.91[f]	11.49[f]	11.79[f]
	8.93[g]	9.70[g]	10.01[g]	11.41[g]	11.72[g]
	Cyt_3 8.516 (0.816)	9.595 (0.802)	9.905 (0.807)	11.382 (0.792)	11.707 (0.792)
	8.40[e]	9.42[e]	9.80[e]	11.33[e]	11.60[e]
	8.64[f]	9.66[f]	10.00[f]	11.53[f]	11.76[f]
	8.91[g]	9.66[g]	10.15[g]	11.45[g]	11.66[g]
	Cyt_4 8.664 (0.798)	9.814 (0.796)	10.008 (0.755)	10.648 (0.774)	13.094 (0.757)
	8.29[e]	9.31[e]	9.89[e]	10.57[e]	12.28[e]
	8.67[f]	9.81[f]	10.36[f]	11.10[f]	12.65[f]
	8.81[g]	9.93[g]	10.07[g]	10.97[g]	12.60[g]
	8.820[b]	9.450[b]	9.900[b]	?[b]	11.8[b]
BA	10.523 (0.771)	11.163 (0.776)	11.401 (0.785)	11.715 (0.765)	11.831 (0.755)
	10.40[b]	11.05[b]	?[b]	11.450[b]	?[b]
menadione	9.223 (0.784)	9.275 (0.785)	9.392 (0.750)	9.935 (0.779)	13.275 (0.711)
	9.51[b]	?	?	?	?
β-carotene	7.65[b]	8.25[b]	8.65[b]	-	-
	7-*cis* 5.332 (0.898)	6.366 (0.880)	7.248 (0.845)	7.950 (0.841)	8.275 (0.853)
	9-*cis* 5.316 (0.901)	6.385 (0.880)	7.248 (0.856)	7.888 (0.842)	8.297 (0.827)
	11-*cis* 5.302 (0.898)	6.321 (0.881)	7.190 (0.849)	7.896 (0.829)	8.332 (0.823)
	13-*cis* 5.358 (0.899)	6.340 (0.888)	7.184 (0.856)	7.919 (0.841)	8.335 (0.832)
	15-*cis* 5.387 (0.900)	6.347 (0.891)	7.217 (0.858)	7.928 (0.848)	8.356 (0.833)
	13,15-*dicis* 5.419 (0.899)	6.343 (0.892)	7.198 (0.859)	7.926 (0.852)	8.343 (0.837)
	7,13′-*dicis* 5.38 (0.900)	6.384 (0.886)	7.252 (0.852)	7.960 (0.852)	8.280 (0.854)

[a]The vertical ionization energies of β-carotene isomers were calculated at the SAC-CI SD-R/6-31+G(d). The numbers in parentheses show the intensity of each ionization band calculated in this work. [b]The experimental values of ionization energies taken form ref 6. [c]Reference 53. [d]Reference 54. [e]Calculated based on the ADC(3) method and 6-31G basis set (ref 63). [f]Calculated based on the OVGF method and 6-311++G(d,p) basis set (ref 63). [g]Calculated based on the P3 method and 6-311G(d,p) basis set (ref 64).

and a NH_2 group. Table S1 (in the Supporting Information) compares the calculated ionization energies (this work) with the experimental results[44] taken from the literature. The average absolute deviation (AAD) from the experimental data is about 0.19 eV which shows that there is a good agreement between theory and experiment. The reason for the energy difference between the calculation and theory can be attributed to the size and incompleteness of the basis set used in the SAC-CI calculations, the basis set and theoretical level which are used for the geometry optimization of molecule, and the intrinsic error which is present in the SAC-CI calculations. However, it is seen that the SAC-CI general-R method in combination with the 6-31+G(d) basis set can quite accurately predict the relative energies of the photoelectron lines of aniline molecule.

dx.doi.org/10.1021/jp311213c | J. Phys. Chem. B XXXX, XXX, XXX−XXX

3. RESULTS AND DISCUSSION

In this section, photoelectron spectra of the considered biological molecules are calculated, assigned, and compared with the experimental results. The photoelectron spectrum of each conformer/tautomer is produced by convoluting the discrete photoelectron bands with the Gaussian distribution function. The same Gaussian width (500 meV; full width at half-maximum) is considered for all the photoelectron bands. All ionization energies are collected in Table 1 and compared with the experimental values taken from the literature. Assignment of the individual photoelectron spectra is also discussed in the following sections.

3.1. 2,4-Dinitrophenol (DNP) and 2,4-Dinitroanisole (DNAN). Nitrophenols belong to a class of nitro compounds most of which are known as explosives, and are often classified as secondary explosives, but some of them such as *m*- and *p*-nitrophenol are common laboratory indicators. Among these compounds, DNP is used as a chemical intermediate for producing of azo dyes, wood preservatives, and pesticides.[45] DNAN is industrially used as an ingredient for production of dyes. Nowadays, DNAN is also used predominantly as an ingredient in explosive formulations.[46]

The experimental He-I photoelectron spectra of DNP[6] and DNAN[6] are shown in Figure 1. The parts of the experimental spectrum of DNP and DNAN (below 12 eV) which are formed from three features are similar. This similarity indicates that the region of spectrum originates from the part of the molecule which is common in DNP and DNAN. The calculated vertical ionization energies of DNP and DNAN (up to 13 eV) are tabulated in Table 1 and compared with the corresponding experimental values. The calculated spectrum of DNP and DNAN was shifted about +0.158 and +0.373 eV, respectively, to match the first feature of the theoretical spectrum with the corresponding feature in the experimental spectrum. As can be seen, relative intensities and energy positions of the features in the calculated spectrum of DNP and DNAN are in very good agreement with those in their experimental spectra.

Based on the theoretical calculations (vertical lines in Figure 1), the first and second features in the experimental photoelectron spectra of DNP and DNAN are only related to the first and second ionization bands, respectively. The third feature is related to three overlapping ionization bands based on the calculations. Therefore, it is difficult to estimate the third, fourth, and fifth vertical ionization energies from this feature without theoretical calculations. As seen in Table 1, the same experimental values were reported for the fourth and fifth ionization energies of DNP and DNAN by Dougherty et al.[6] while the calculated energy difference between the fourth and fifth ionization bands of DNP and DNAN are 0.397 and 0.176 eV, respectively.

Tables S2 and S3 (in the Supporting Information) report the main electronic configurations of each ionic state obtained from the SAC-CI general-R calculations for DNP and DNAN, respectively. Contribution of the dominant natural bonding orbitals (NBOs) in each ionized orbital obtained from the NBO calculations at the Hartree−Fock (HF)/6-31+G(d) level of theory is also reported in Tables S2 and S3. It is evident that the main electronic configurations, contributing to the wave function of each ionic state for both DNP and DNAN, are mostly related to the one-electron ionization process and there is no contribution from the electronic configurations related to satellite processes (shakeup and shake-off) because the ionized

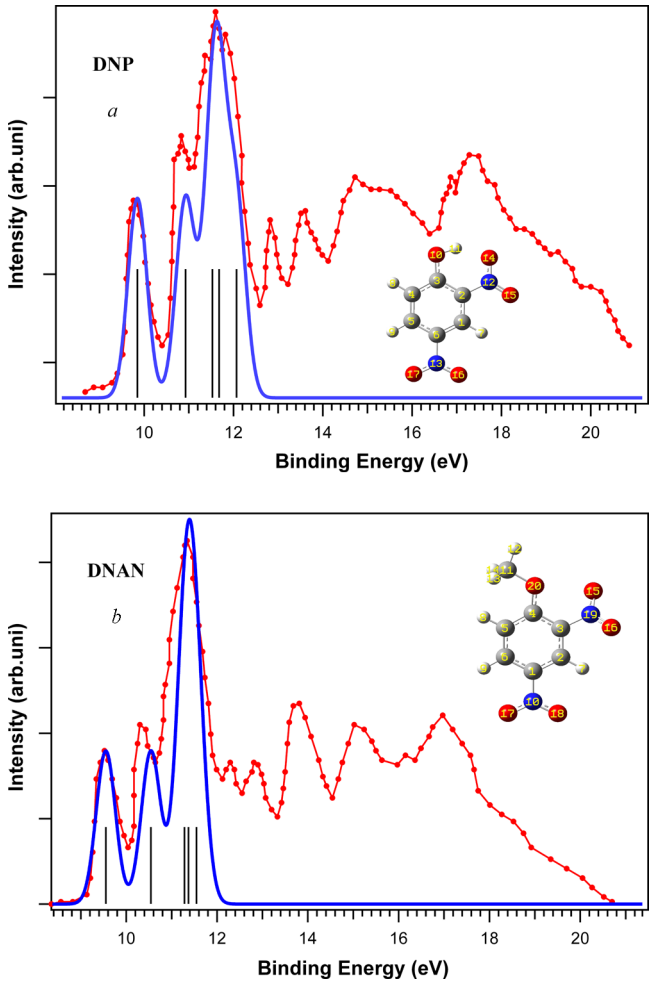

Figure 1. Experimental He-I photoelectron spectra of (a) 2,4-dinitrophenol (DNP) (red point line) and (b) 2,4-dinitroanisole (DNAN) (red point line) taken from ref 6 compared with their corresponding theoretical photoelectron spectra (solid blue line) calculated in this work at the SAC-CI general-R/6-31+G(d) level of theory. Vertical lines show energy positions of the calculated ionization bands. The calculated spectra of DNP and DNAN have been shifted about +0.158 and +0.373 eV, respectively.

electrons come from the outer valence region of the molecule. In the shakeup process, the core electron is ionized (K-shell ionization) and the ionized electron interacts with the one valence electron and excites it (shakes it up) to a higher energy level and finally there are two holes in the electronic configuration of atom or molecule, one because of the ionized electron and the another due to the excited electron (1 hole and 1 photoelectron). Sometimes, the ionized electron interacts with the two electrons in the valence region and simultaneously excites them to the higher unoccupied orbitals (2 holes and 1 photoelectron). In the shake-off process, one or two electrons are ejected from the K-shell ionized molecule.

Comparison of Table S3 with Table S2 shows that the amount of electron correlations for DNAN is more than that of DNP because the main configuration of the third and fifth ionic states of DNAN are a linear combination of the one-electron ionization determinants. In addition, it is evident that the energy order of the photoelectron bands which was calculated at the SAC-CI level of theory is different from the order

dx.doi.org/10.1021/jp311213c | J. Phys. Chem. B XXXX, XXX, XXX−XXX

predicted by Koopman's theorem[47] based on the energy order of molecular orbitals.

NBO calculations showed that the first and second ionization bands of DNP and DNAN were mostly related to the ionization from the highest occupied molecular orbital (HOMO) and HOMO-1. These molecular orbitals were related to the π-molecular orbitals of the C═C bonds of the benzene ring (Tables S2 and S3). NBO calculations also demonstrated a small contribution from the lone pair of the oxygen atom of −OH and $-OCH_3$ groups in the HOMO of DNP and DNAD, respectively. It is expected that the natural bonding orbitals contributing to the first and second ionization bands of DNP and DNAN are similar to those of phenol.[48,49] Therefore, the first and second ionization events of DNP and DNAN correlate directly with similar events in phenol. The third ionization band of DNP and DNAN was due to the lone pair of oxygen of NO_2 groups (Tables S2 and S3). Similarly, the fourth ionization band of DNP and DNAN was related to the lone pair of oxygen of NO_2 groups; however, there was some contribution from the π-molecular orbital of the N═O bond. It can be concluded that the third feature in the photoelectron spectra of DNP and DNAN is only related to the ionization of the NO_2 group which can be also seen in the photoelectron spectrum of nitrobenzene.[50]

3.2. Nicotinic Acid (NA) and Nicotinic Acid Methyl Ester (NAME). NA or vitamin B_3 is a vital nutrient for humans and animals and is widely used as an additive in food, forage, and cosmetics.[51] NAME is used as a rubefacient for the treating of a variety of diseases such as respiratory ones.[52]

Figures 2 and 3 show the experimental photoelectron spectra of NA and NAME, taken from ref 6, respectively. As shown in Figure 2, there are two rotational conformers for NA, which are denoted NA_1 and NA_2 in this work. To obtain the Boltzmann population ratios of these two conformers, at the temperature which was used by Dougherty et al.[6] for evaporating the sample (300 °C), thermochemistry calculations were performed at the B3LYP/aug-cc-pVDZ level of theory. The calculated values of Gibbs free energies of conformers were used to obtain their population ratios. The calculated population ratios of NA_1 and NA_2 were 0.492 and 0.487, respectively. Similar to NA, there were two rotational conformers for NAME; but, the population ratio of one of them (oxygen of the carbonyl group is in the trans position relative to carbon number 2) was considerably higher than that of the other (>90). Therefore, it is expected that the photoelectron spectrum of NAME is only dominated by one conformer. The molecular structure of the most stable conformer of NAME has also been shown in Figure 3.

Figure 2 also shows the calculated photoelectron spectra of the conformers of NA (up to 18 eV) calculated at the SAC-CI general-R method using 6-31+G(d) basis set. As can be observed, there are seven vertical ionization bands for the NA_1 conformer in the range of 9−17 eV while the number of ionization bands reaches 12 ionization bands for NA_2 in this energy range. Rotation of the COOH group around the C−C bond changes the electronic correlation energy so that the number of ionic states of the NA_2 conformer accessible in the considered binding energy increases in comparison with the NA_1 conformer. To calculate the photoelectron spectra of NA and NAME (blue traces in Figures 2 and 3), the spectra of individual conformers which were weighted by their population ratio were summed. As shown, there is good agreement between the theoretical spectra of NA and NAME and their corresponding experimental spectra. The calculated spectra of

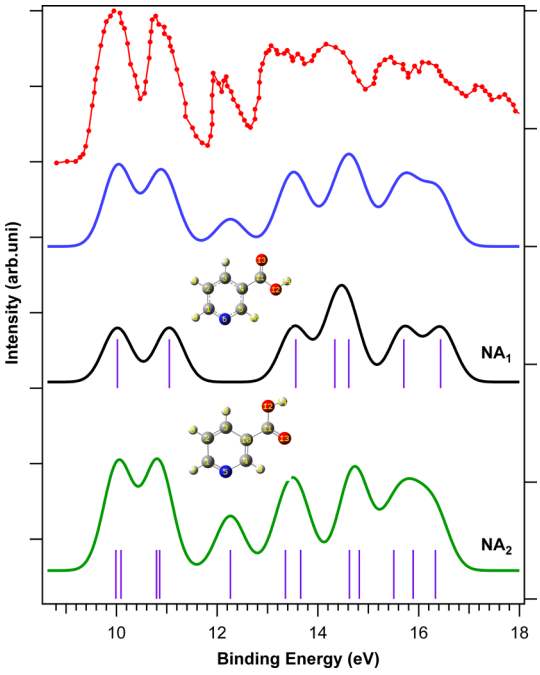

Figure 2. Experimental He-I photoelectron spectrum of nicotinic acid (NA) (red point line) taken from ref 6 compared with its corresponding theoretical Boltzmann-weighted ($0.492NA_1$ + $0.487NA_2$) photoelectron spectrum (solid blue line) calculated in this work at the SAC-CI general-R/6-31+G(d) level of theory. Black and green traces indicate the calculated photoelectron spectra of NA conformers (NA_1 and NA_2) calculated at the SAC-CI general-R/6-31+G(d) level of theory, respectively. Vertical lines show energy positions of the calculated ionization bands. The calculated spectrum of NA and its conformers has been shifted about +0.631 eV.

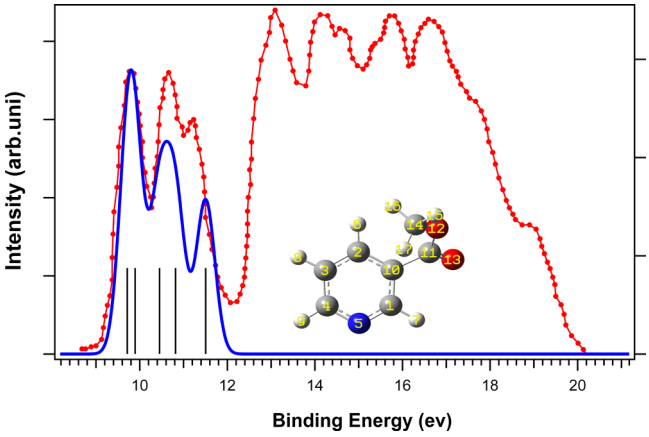

Figure 3. Experimental He-I photoelectron spectrum of nicotinic acid methyl ester (NAME) (red point line) taken from ref 6 compared with its corresponding theoretical photoelectron spectrum (solid blue line) calculated in this work at the SAC-CI general-R/6-31+G(d) level of theory. Vertical lines demonstrate the energy positions of the calculated ionization bands. The calculated spectrum of NAME has been shifted about +0.183 eV.

NA and NAME (blue traces in Figures 2 and 3) were shifted about 0.631 and 0.183 eV, respectively, to match the first feature of the calculated spectrum with the experimental one. Comparison of the experimental spectrum of NA with the calculated spectra of NA_1 and NA_2 shows that the third feature, located around 12.251 eV binding energy in the experimental

dx.doi.org/10.1021/jp311213c | J. Phys. Chem. B XXXX, XXX, XXX−XXX

spectrum, only originated from the NA_2 conformer. This observation is very important when one prefers to selectively trace NA_2 conformer in a process using photoelectron spectroscopy.

The calculated vertical ionization energies of NA and NAME are reported in Table 1. As seen, the calculated first ionization energies of the NA_1 and NA_2 conformers are almost equal to each other. The first ionization energy of NA which is obtained using the electron-impact ionization technique is about 9.61 eV[53] and is in good agreement with the calculated value in this work. The experimental second to fifth ionization energies of NA (Table 1) reported by Dougherty et al.[6] are close to those calculated for the NA_2 conformer in the present work. The calculated first ionization energy of NAME is about 9.53 eV which is in good agreement with the experimental value (9.9 ± 0.1) reported by Stefanović et al.[54]

The main electronic configurations of the calculated ionic states of NA obtained from the SAC-CI general-R calculations as well as the contribution of the dominant natural bonding orbitals (NBOs) of the relevant ionized molecular orbitals obtained from the NBO calculations at the HF/6-31+G(d) level of theory are given in Tables S4 and S5 (in the Supporting Information). The first ionization band of NA_1 and NA_2 was due to the ionization from the molecular orbital no. 32 related to the π-molecular orbitals of C═C bonds of the pyridine ring. The second ionization band of NA_1 and NA_2 was due to the ionization from the molecular orbital no. 29 and 30, respectively. The dominant natural bonding orbitals contributing to the orbital no. 29 of NA_1 were only related to the lone pair of the oxygen of the C═O bond. The molecular orbital no. 30 of NA_2 was only due to the lone pair of nitrogen. It can be seen that the rotation around the C−C bond for converting the NA_1 to NA_2 completely changes the nature of the second ionization band in NA_2 compared with NA_1. The third ionization band of NA_1 originated from the π-molecular orbital of C═O bond and the lone pair of oxygen (O−H) while it originated from the π-molecular orbitals of C═C and C═N of the pyridine ring for NA_2. Similar discussion can be presented for the fourth and fifth ionization bands of NA_1 and NA_2 conformers which are not further discussed here. It is worth noting that the main configuration of the ionic states of NA_1 and NA_2 reported in Tables S4 and S5 is mainly composed of the one-electron ionization determinants.

Similarly, Table S6 (in the Supporting Information) reports NBO results of the most stable conformer of NAME. Similar to NA, the first ionization band of NAME was due to the ionization of the π-molecular orbital of the C═C bond of the pyridine ring. The second ionization band was related to the ionization from the molecular orbital no. 34 which has the nonbonding character due to the lone pair of nitrogen (similar to NA_2). The natural bonding orbital character of the molecular orbitals no. 35, 33, and 32 of NAME (related to the third, fourth, and fifth ionization band) were similar to the corresponding molecular orbitals in NA_2. It is evident from Table 1 that the replacement of H of the OH group with the CH_3 group shifts the position of the ionization bands of NAME to the lower binding energy compared to NA_2.

3.3. Nicotinamide (NAM) and *N*,*N*-Diethylnicotinamide (DNAM). NAM is the most common form of the vitamin B_3 which has antipellagra activity. It is found in the body as a part of nicotinamide adenine dinucleotide and participates in a wide range of biological processes including production of energy, synthesis of fatty acids, cholesterol steroids, signal transduction, and maintenance of integrity of the genome. It has been also found to inhibit reactive-oxygen-species-induced apoptosis, inhibit phagocytic generation of reactive oxygen species, scavenge reactive oxygen species, and inhibit the oxidative activity of nitric oxide. NAM also exhibits antioxidant, anti-inflammatory, and anticarcinogenic activities as well as putative activity against osteoarthritis and granuloma annulare.[55,56] DNAM, one of the respiratory central stimulants, is used to treat respiratory failure in clinical practice. Meanwhile, DNAM is one of the abused drugs which are banned for athletes.

Figure 4 shows the He-I photoelectron spectrum of NAM[6] as well as its calculated spectrum obtained in this work. As shown,

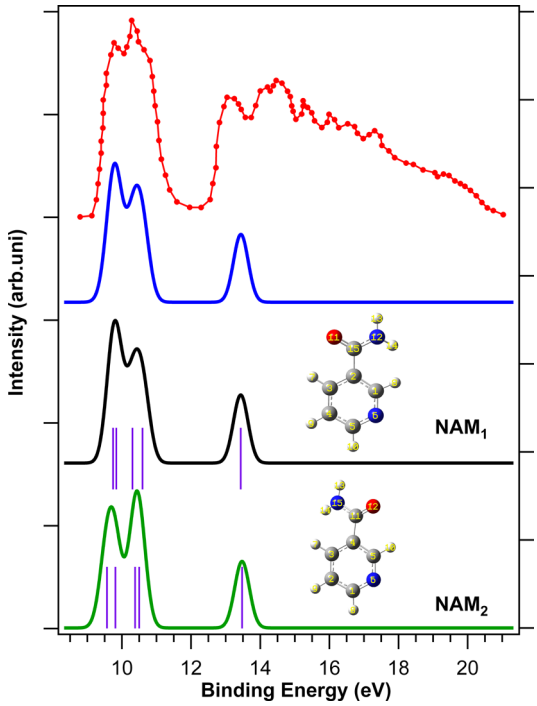

Figure 4. Experimental He-I photoelectron spectrum of nicotinamide (NAM) (red point line) taken from ref 6 compared with its corresponding theoretical Boltzmann-weighted ($0.76NAM_1$ + $0.24NAM_2$) photoelectron spectrum (solid blue line) calculated in this work at the SAC-CI general-R/6-31+G(d) level of theory. Black and green traces show photoelectron spectra of NAM conformers (NAM_1 and NAM_2) calculated at the SAC-CI general-R/6-31+G(d) level of theory, respectively. Vertical lines show energy positions of the calculated ionization bands for both conformers. The calculated spectra of NAM and its conformers have been shifted about +0.33 eV.

there are two conformers for NAM (NAM_1 and NAM_2). The Boltzmann population ratio of NAM_1 and NAM_2 obtained from the thermochemistry calculations at the B3LYP/aug-cc-pVDZ level of theory were 0.76 and 0.24, respectively. Therefore, it is expected that the experimental photoelectron spectrum of NAM is mostly dominated by the NAM_1 conformer. It is evident from Figure 4 that the calculated photoelectron spectra of NAM_1 and NAM_2 conformers are very similar in the considered binding energy region. As seen in Figure 4, there is very good agreement between the calculated photoelectron spectrum of NAM (blue trace) and the experimental spectrum. The calculated spectrum of NAM was shifted as +0.33 eV to match its first feature with the corresponding feature in the experimental spectrum. The first

dx.doi.org/10.1021/jp311213c | J. Phys. Chem. B XXXX, XXX, XXX−XXX

and second features in the calculated spectra of NAM_1 and NAM_2 were composed of two ionization bands while the third feature was related to only one ionization band.

Table 1 compares the calculated vertical ionization energies of NAM with the corresponding experimental results. The experimental value of the fifth ionization energy of NAM, reported by Dougherty et al.[6] is considerably different (about 2.3 eV) from its calculated value in this work. Therefore, it is expected that the reported experimental value of the fifth ionization energy of NAM is not reasonable. The calculated first ionization energies of NAM_1 and NAM_2 are 9.414 and 9.237 eV, respectively.

Tables S7 and S8 (in the Supporting Information) report the main electronic configurations contributing in the wave function of the involved ionic states, as well as the NBO result for the NAM_1 and NAM_2 conformers, respectively. Due to the difference in the amount of electron correlations in the two conformers, the kind of single ionized determinants, contributing to the main configuration of the same ionization bands is different in the two conformers. For example, the first ionization band of NAM_1 is related to the ionization from the molecular orbitals no. 32 and 29 while it changes to a linear combination of molecular orbitals no. 32 and 30 in NAM_2.

The first ionization band of NAM_1 is related to the ionization from π-molecular orbital of the pyridine ring (π(C1═C2), the lone pairs of oxygen of the carbonyl group, and the nitrogen of the C_5H_4N ring. The natural bonding orbitals contributing to the first ionization band of NAM_2 is the same as those of NAM_1 except that there is no contribution from the lone pair of the oxygen of C═O group. The main single ionized molecular orbitals contributing to the wave function of the second ionic state of NAM_1 are similar to the first ionization band. The second ionization band of NAM_2 is composed of linear combination of three one-electron ionization determinants of molecular orbitals 30, 32, and 29. The molecular orbital no. 29 of NAM2 has the lone pair character originating from the N of NH_2 and C_5H_4N groups. The third ionization band of NAM_1 originates from the ionization of molecular orbitals no. 31, 29, and 30. The natural bonding orbitals of molecular orbital no. 31 are related to the π(C3−C4) and π(C5−N6) of the pyridine ring. The natural bonding orbitals of molecular orbital no. 30 of NAM_1 are the lone pair of nitrogen of NH_2 group and π(C═O). The third ionization band of NAM_2 molecule is only related to the ionization from the lone pairs of N (NH_2 and C_5H_4N) and O (C═O). The fourth and fifth ionization bands of NAM_1 and NAM_2 mostly originate from π-molecular orbitals of pyridine ring (C═C and C═N), the lone pairs of the oxygen of C═O, nitrogen of C_5H_4N (for NAM_1) and NH_2 (for NAM_2). The difference between the NAM and NA molecules (previous section) is related to replacing of OH with NH_2 group in NA molecule. Comparison of the main electronic configurations of the ionic states of NAM with NA shows that replacing OH with NH_2 group increases the amount of the electron correlations in the molecule so that the ionic wave functions of NAM are a linear combinations of the one-electron ionization determinants.

Figure 5 demonstrates the He-I photoelectron spectrum of DNAM[6] along with the calculated photoelectron spectra of its conformers. Similar to NAM, there were two conformers for DNAM ($DNAM_1$ and $DNAM_2$) with 0.185 and 0.815 population ratios, respectively. It can be seen that the population ratios of conformers are reversed for DNAM in comparison with NAM. According to Figure 5, the calculated

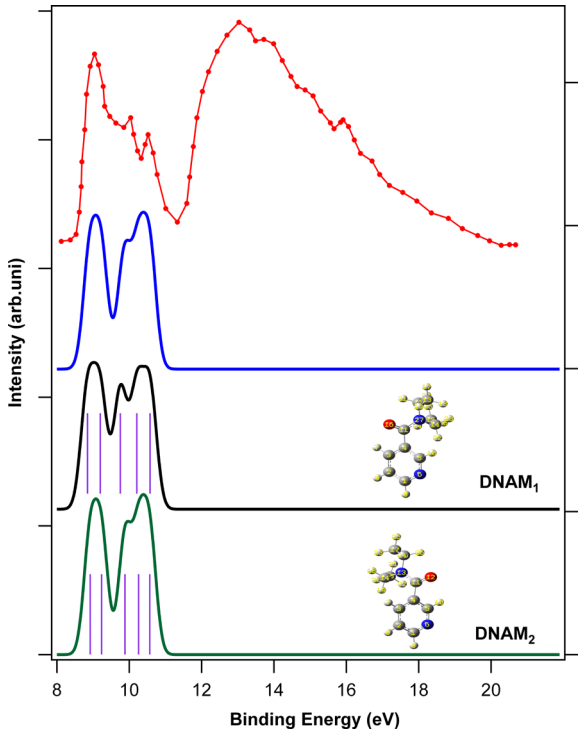

Figure 5. Experimental He-I photoelectron spectrum of *N*,*N*-diethylnicotinamide (DNAM) (red point line) taken from ref 6 compared with its corresponding theoretical Boltzmann-weighted (0.185$DNAM_1$ + 0.815$DNAM_2$) photoelectron spectrum (solid blue line) calculated in this work at the SAC-CI general-R/6-31+G(d) level of theory. Black and green traces show photoelectron spectra of DNAM conformers ($DNAM_1$ and $DNAM_2$) calculated at the SAC-CI general-R/6-31+G(d) level of theory, respectively. Vertical lines demonstrate the energy positions of the calculated ionization bands for both conformers. The calculated spectra of DNAM and its conformers have been shifted about +0.900 eV.

photoelectron spectra of $DNAM_1$ and $DNAM_2$ are very similar. The calculated photoelectron spectra of DNAM and its conformers were shifted as +900 meV in order to match the first feature of the theoretical spectrum (blue trace in Figure 5) with the corresponding feature in the experimental spectrum. Relative energy positions of the features in the calculated spectrum are in good agreement with those in the experiment spectrum. There is no report on the first vertical ionization energy of DNAM in the literature. Dougherty et al.[6] reported the value for the point at which the ionization event was initiated (8.65 eV). The first vertical ionization energies of $DNAM_1$ and $DNAM_2$, considering a +900 meV shifting in the theoretical spectrum, are 8.846 and 8.920 eV, respectively.

Tables S9 and S10 (in the Supporting Information) report the main electronic configurations contributing to the wave functions of the related ionic states of the DNAM conformers as well as their NBO result. The first ionization bands of $DNAM_1$ and $DNAM_2$ are mostly due to the ionization from the molecular orbital no. 47. The molecular orbital no. 48 is HOMO at the HF level of theory for both $DNAM_1$ and $DNAM_2$ while, at the SAC-CI general-R level of theory, the energy order of these molecular orbitals is reversed because of the electronic correlations. The natural bonding orbitals contributing in the molecular orbital no. 47 of both $DNAM_1$ and $DNAM_2$ are mostly due to the lone pair of N of CON group. The main configuration of the ionic state of the second

dx.doi.org/10.1021/jp311213c | J. Phys. Chem. B XXXX, XXX, XXX−XXX

ionization band of $DNAM_1$ is related to ionization from the π-molecular orbitals of pyridine ring (π(C═C), π(C═N)), lone pairs of the N of the pyridine ring and O of C═O bond. The natural bonding orbitals of the second ionization band of $DNAM_2$ are similar to those of $DNAM_1$, except that there are some contributions from the π-molecular orbital of (C═O) and lone pair of N of (CON). Assignment of the rest of the ionization bands of DNAM conformers can be deduced from Tables S9 and S10 and is not further discussed here.

3.4. Barbituric Acid (BA). BA is widely used in manufacturing plastics, dyes, polymers,[57,58] and textiles, and in pharmaceutical preparations of barbiturates.[59] BA is not a hypnotic in itself but its derivatives show high hypnotic and sedative action and are usually used as hypnotics, sedatives, anticonvulsants, and anesthetics. BA exists only in the keto form.[60]

Figure 6 shows its experimental spectrum recorded by Dougherty et al.[6] and compares it with its calculated spectrum

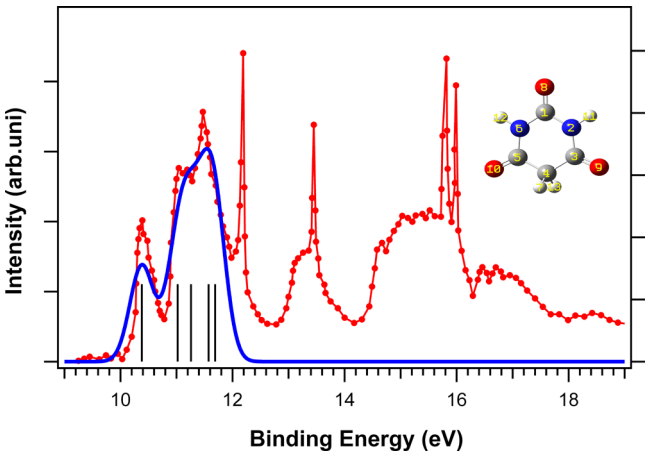

Figure 6. Experimental He-I photoelectron spectrum of barbituric acid (BA) (red point line) taken from ref 6 compared with its corresponding theoretical photoelectron spectrum (solid blue line), calculated in this work at the SAC-CI general-R/6-31+G(d) level of theory. Vertical lines show energy positions of the calculated ionization bands. The calculated spectrum of BA has been shifted about −0.142 eV.

(this work). The calculated photoelectron spectrum was shifted about −0.142 eV to adjust energy position of the first feature with that in the experimental spectrum. As seen, there is an excellent agreement between the calculated and experimental spectrum. Barbituric acid belongs to the C_2 symmetry group and its ionic electronic states can be classified as A and B which are irreducible representations of C_2 symmetry group. Vertical ionization energies of barbituric acid are presented in Table 1 and compared with the experimental results.[6] The calculations showed that the first feature in the experimental spectrum was only due to the first ionization band. The first ionization band was due to the ionization from the molecular orbital no. 32 which was mostly related to the ionization of lone pairs of oxygen atoms of the carbonyl group in the molecule (Table S11 in the Supporting Information). The second feature was composed of the two ionization bands. These two ionization bands were related to the ionization form the molecular orbitals no. 33 and 27 which were due to the lone pairs of nitrogen and the π-molecular orbital of C═O bonds. The fourth ionization band was due to the ionization from the molecular orbital no. 22, the NBO character of which was similar to the first ionization band. It is evident that Koopmans' theorem does not apply for barbituric acid. It is important to notice that the main electronic configuration of each ionization band is only due to the one-electron-ionized determinant.

3.5. Cytosine (Cyt). Cytosine can be found as a part of DNA, a part of RNA, or a part of a nucleotide. As cytidine triphosphate (CTP), it can act as a cofactor to enzymes and can transfer a phosphate to convert adenosine diphosphate (ADP) into adenosine triphosphate (ATP).[61]

Several valence photoelectron spectra of cytosine have been reported in the literature.[6,7,62,63] Dougherty et al.[6] and Yu et al.[62] recorded He-I photoelectron spectrum of cytosine in the gas phase, separately. In another study, angle-resolved outer valence photoelectron spectrum of cytosine was recorded using synchrotron radiation.[63] The valence ionization energies of cytosine have been also studied theoretically. For example, Dolgunicheva et al. calculated the ionization energies of cytosine using partial third-order method (P3).[64] Similarly, Trofimov et al. used the third-order algebraic−diagrammatic construction approximation scheme (ADC(3)) (using 6-31G basis set) and outer-valence Green's function (OVGF) (using 6-31G and 6-311++G(d,p) basis sets), separately, to calculate and assign photoelectron spectra of four tautomers of cytosine.[63]

Two experimental He-I photoelectron spectra of cytosine[6,62] are shown in Figure 7. Also, the theoretical spectra of four tautomers/conformers of cytosine which where calculated in this work are included in Figure 7 and compared with the corresponding theoretical spectra calculated using the ADC(3) method which was taken from ref 63. To calculate the theoretical spectrum of cytosine, the Boltzmann population ratio of tautomers/conformers calculated by Fogarasi[65] was used. The population ratio of Cyt_1, Cyt_2, Cyt_3, and Cyt_4 at the temperature appropriate with the experimental photoelectron spectra was 0.22, 0.38, 0.17, and 0.24, respectively. It is clear that the conformer Cyt_2 is the most stable form of cytosine and its photoelectron spectrum should to a large extent determine the overall spectral profile of composite spectrum. The Boltzmann-weighted sum of the individual spectra representing Cyt_1, Cyt_2, Cyt_3, and Cyt_4 forms is also separately shown in Figure 7 for general-R SAC-CI and ADC(3) calculations. In addition, vertical ionization energies of the tautomers/conformers of cytosine are also tabulated in Table 1 and compared with the corresponding theoretical values taken from refs 63 and 64.

There are two differences between the two experimental spectra of Cyt, as shown in Figure 7. The first difference is related to relative intensity of the first two features in the two spectra. The intensities of these two features are nearly equal in the spectrum recorded by Dougherty et al.[6] while the intensity of the first feature is lower than the second one in the spectrum recorded by Yu et al.[62] The second difference is related to the relative energy positions of the corresponding features in the two spectra. The features of Yu et al.'s spectrum are located at the higher binding energy in comparison with the corresponding features in the spectrum of Dougherty et al.[6] It is seen that the relative intensity of the first to second feature in the experimental spectrum of Yu et al.[62] is in good agreement with what is seen in the calculated spectrum (blue trace in Figure 7). Also, it is evident that the relative energy positions of the features in the experimental spectrum of Yu et al.[62] are more consistent with the theory than those in the spectrum of

dx.doi.org/10.1021/jp311213c | J. Phys. Chem. B XXXX, XXX, XXX−XXX

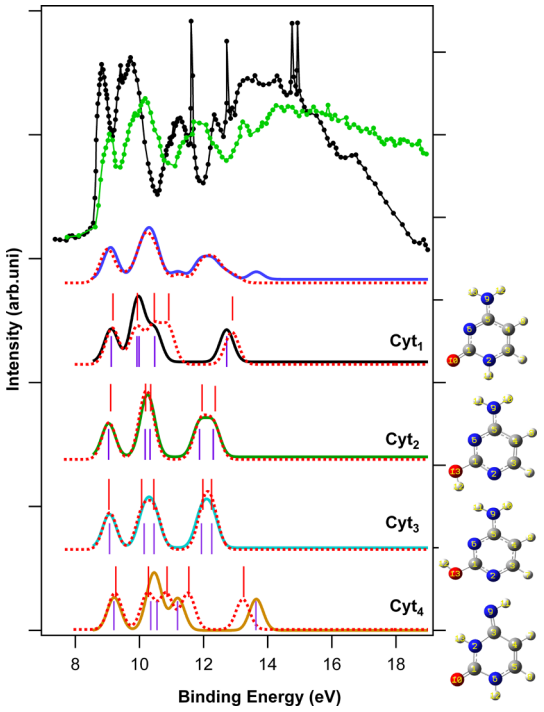

Figure 7. Experimental He-I photoelectron spectra of cytosine (Cyt) (black point line and green point line) taken from refs 6 and 62, respectively, compared with its corresponding theoretical Boltzmann-weighted photoelectron spectrum (solid blue line), calculated in this work at the SAC-CI general-R/6-31+G(d) level of theory. The black, green, turquoise, and brown solids lines show photoelectron spectra of Cyt tautomers (Cyt_1, Cyt_2, Cyt_3, and Cyt_4), calculated at the SAC-CI general-R/6-31+G(d) level of theory, respectively. The red dashed lines show the calculated Boltzmann-weighted photoelectron spectrum of Cyt and the photoelectron spectra of its tautomers, taken from ref 62, calculated using ADC(3) method. The lavender and red vertical lines show energy positions of the ionization bands calculated in this work and taken from ref 62, respectively. The SAC-CI and ADC spectra of cytosine were shifted about 550 and 670 meV, respectively.

Dougherty et al.[6] For example, the energy difference between the first and third feature in the Yu et al.'s and Dougherty et al.'s spectra are 2.81 and 2.45 eV, respectively. The corresponding values which were calculated at the SAC-CI and ADC(3)[63] levels of theory are 2.90 and 3.1 eV, respectively. It can be concluded that the photoelectron spectrum recorded by Yu et al. is more accurate and reliable than other experimental spectrum. It should be mentioned that the calculated spectra at the SAC-CI and ADC(3) (taken from ref 62) levels of theory were shifted about 550 and 670 meV, respectively, to match their first features with the corresponding feature in the experimental spectrum recorded by Yu et al.[62]

Change in the transmission of the electron analyzer during the measurement because of the sample depositing on its slits and lenses is one of the factors that affects relative intensity of features of the recorded photoelectron spectrum. To avoid this problem, it is necessary to keep the chamber and the electron analyzer warm during the experiment to prevent deposition of the sample. Also, charging the deposited sample due to the electrons produced by photoionization changes the kinetic energy of the electrons and causes the relative energy positions of the features in the spectrum to be inconsistent with reality. The authors believe that these two problems may have occurred for the spectrum of cytosine reported by Dougherty et al.[6]

It is evident from Figure 7 that the spectra of Cyt_2 and Cyt_3, calculated at the SAC-CI general-R level of theory, are same as those calculated using the ADC(3) method taken from ref 63. There are some differences between the calculated spectra at the SAC-CI and ADC(3) levels of theory for Cyt_1 and Cyt_4 tautomers. Comparison of the calculated photoelectron spectrum of Cyt (blue trace in Figure 7) with the experimental spectrum of Yu et al.[62] shows that the third feature in the photoelectron spectrum of cytosine is only due to the Cyt_2 and Cyt_3 tautomers and the fourth one is only due to the Cyt_4 tautomer. It can be seen in Figure 7 that the SAC-CI general-R level of theory can predict the fourth feature in the experimental spectrum compared to ADC(3) level of theory.

Tables S12 and S13 (in the Supporting Information) report the main electronic configurations contributing to the wave function of the ionic states of Cyt_1 and Cyt_2, respectively. The natural bonding orbitals of each ionized orbital are also reported. As shown in Figure 7, the first feature of the calculated spectrum of each tautomer/conformer of cytosine is due to only one ionization band. The first ionization band of both Cyt_1 and Cyt_2 is related to the ionization from orbital no. 29. The natural bonding character of this orbital is mostly related to π(C═C), π(C═N) and partially related to the lone pairs of N ($C_4H_3N_2$) and N(NH_2) groups for both Cyt_1 and Cyt_2. The second ionization band of Cyt_1 is due to the ionization from orbital no. 28 while it is from orbital no. 27 for Cyt_2. It is seen that the energy order of molecular orbitals no. 27 and 28 is reversed in Cyt_2 because of the difference in the electronic correlation compared to Cyt_1. The molecular orbital no. 28 of Cyt_1 is related to the lone pair of N(NH_2) and π(C═N), and the molecular orbital no. 27 of Cyt_2 is completely related to the lone pair of N of $C_4H_2N_2$. Similar discussion can be explained for the assignment of other ionization bands which can be easily extracted from Tables S12 and S13. These tables demonstrate that the amount of the electronic correlation in Cyt_1 is more than Cyt_2 because of the presence of linear combination of the single ionized determinant for some ionic states.

3.6. Uric Acid (UA). UA is the product of purine metabolism in humans. High levels of this substrate are related to several diseases such as gout, hyperuricemia, and the LeschNyhan syndrome. In addition, UA plays an important role as biochemical risk marker for cardiovascular diseases, metabolic syndrome, and diabetes mellitus. On the other hand, UA is known for its antioxidant properties that arise from its ability to scavenge hydroxyl radicals, singlet oxygen, and oxo-heme oxidants.[66−68]

The molecular structure of UA is similar to that of hypoxanthine and xanthine; but, it has more carbonyl bonds and is stable in keto form. The only reported He-I photoelectron spectrum of uric acid was recorded by Dougherty et al.[6] To the best of the present authors' knowledge, there is no theoretical study on the calculation of valence photoelectron spectrum of UA and comparison with its experimental photoelectron spectrum in the literature. Figure 8 compares the photoelectron spectrum of UA calculated in this work with its experimental spectrum. The calculated photoelectron spectrum was shifted about +0.311 eV to adjust energy position of the first feature with that in the experimental spectrum. As seen, the features of the experimental spectrum in the range of 8−12 eV are related to the five ionization bands of

dx.doi.org/10.1021/jp311213c | J. Phys. Chem. B XXXX, XXX, XXX−XXX

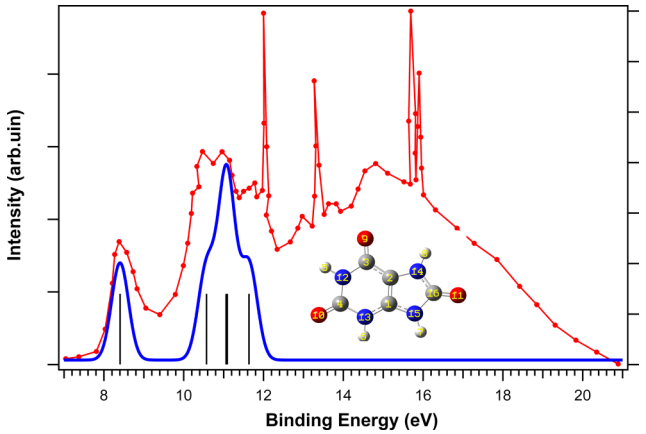

Figure 8. Experimental He-I photoelectron spectrum of uric acid (UA) (red point line), taken from ref 6, compared with its corresponding theoretical photoelectron spectrum (solid blue line) calculated in this work at the SAC-CI general-R/6-31+G(d) level of theory. Vertical lines show energy positions of the calculated ionization bands. The calculated spectra were shifted about +0.311 eV.

the molecule based on the present calculations. The first feature in the experimental spectrum is only related to the first ionization band of UA. The first ionization band is related to the ionization of molecular orbital no. 43 (HOMO). This molecular orbital is mostly related to the lone pairs of the nitrogen atoms, π(C═C) bond (Table S14 in the Supporting Information). The second feature in the experimental spectrum is only related to the second ionization band. The second ionization band is due to the ionization from the molecular orbital no. 41 related to the lone pairs of oxygen atoms of C═O bond. The third and fourth features in the experimental spectrum are related to the two and one ionization bands, respectively. The third ionization band of UA is only due to the ionization from the molecular orbital no. 42 which is mostly related to the lone pair of N12 in the molecule. The fourth ionization band is related to lone pair of O11(C═O) and the fifth one is due to the ionization of the lone pairs of N13 and N15, and π(C═O) bond.

3.7. β-Carotene. β-Carotene is a strongly colored red-orange pigment abundant in plants and fruits and plays an important role in protection from oxidation damage.[69] It is also one of the most important vitamin A precursors. β-Carotene is usually present in nature with all the double bonds in the polyene chain having an all-trans configuration. It has been found that radiation of solutions and heating of the foods may lead to cis isomerization of β-carotene.[70] There are 7-, 9-, 11-, 13-, and 15-*monocis* isomers and different dicis isomers including 7,13′-, 9,13-, 9,13′-, 9,15-, 11,11′-, and 13,15-*dicis*. The stability and the vibrational spectra of β-carotene isomers were investigated by Ceron-Carrasco et al. using DFT calculations.[71] Figure 9 demonstrates the most stable selected isomers of β-carotene which were studied in this work.

The only reported valence photoelectron spectrum of β-carotene in the literature was in the work of Dougherty et al.[6] In this work, the valence photoelectron spectra of the seven most stable isomers of β-carotene including 7-, 9-, 11-, 13-, and 15-*monocis* and 7,13′- and 13,15-*dicis* were calculated (Figure 10). Twenty vertical ionization energies were calculated at the SAC-CI SD-R level of theory (level three) using 6-31+G(d) basis set applied to the optimized structures obtained at the B3LYP/6-31G(d,p) level of theory. It should be mentioned

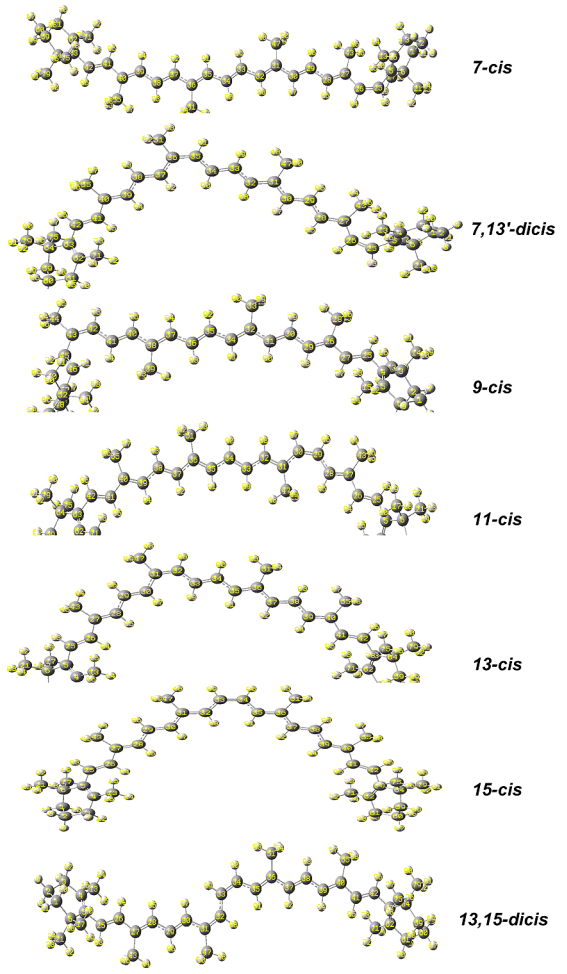

Figure 9. Selected cis isomers of β-carotene considered in this work.

that the general-R version of SAC-CI was not used here because the size of β-carotene is relatively large and the calculation will be so time consuming even while using the 6-31+G(d) basis set.

Table 1 reports the first five vertical ionization energies of the considered isomers of β-carotene. As shown, the vertical ionization energies of the isomers are nearly equal to each other. For example, the difference among the first vertical ionization energies of the isomers is below 100 meV. Also, it is evident from Figure 10 that the calculated photoelectron spectra are very similar to each other which means that the population ratios of isomers do not have any effect on the total photoelectron spectrum of β-carotene.

Figure 11 compares the calculated photoelectron spectrum of β-carotene (up to 12 eV) with the experimental spectrum recorded by Dougherty et al.[6] This comparison shows an energy difference of about 2.17 eV between the first features of the calculated (dashed black line) and experimental spectrum (red trace). Based on the theoretical calculations (Table 1), the first feature of the experimental spectrum is only related to the first ionization bands of the isomers. This energy difference between the positions of the calculated and experimental first ionization band seems to be high. One may think that this high energy difference can be related to the insufficiency of the applied level of theory and size of the basis set. It should be mentioned that the SAC-CI level of theory is one the most accurate theoretical methods in the calculation of outer valence

dx.doi.org/10.1021/jp311213c | J. Phys. Chem. B XXXX, XXX, XXX−XXX

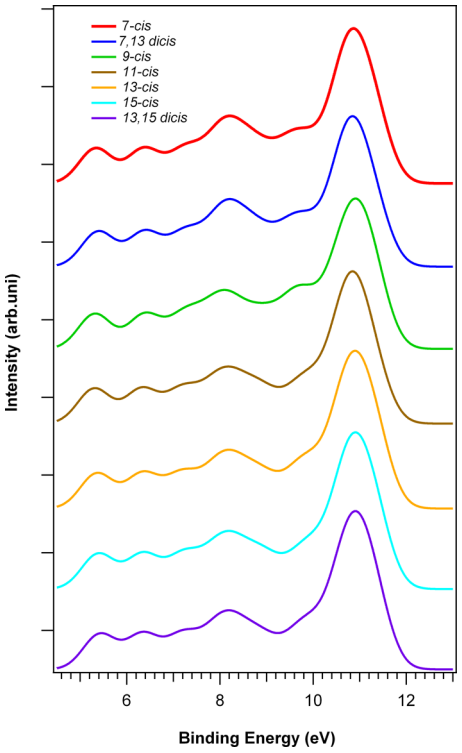

Figure 10. Photoelectron spectra of different isomers of β-carotene, shown in Figure 9, calculated at the SAC-CI SD-R/6-31+G(d) level of theory.

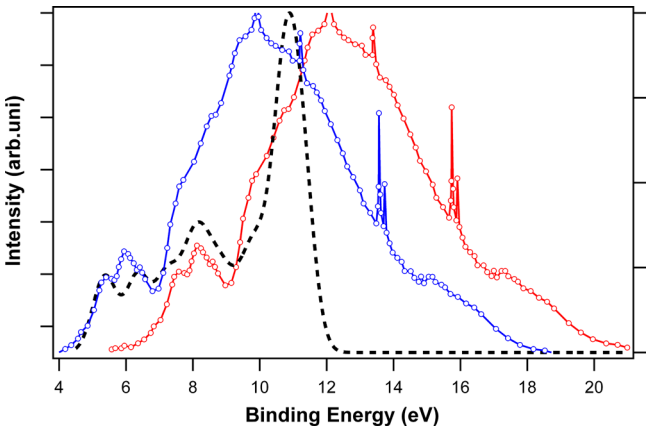

Figure 11. Comparison of photoelectron spectrum of β-carotene (black dashed line) calculated at the SAC-CI SD-R/6-31+G(d) level of theory with its experimental spectrum (red point line) taken from ref 6. The blue trace shows the experimental spectrum of ref 6 which has been shifted about 2.17 eV to lower binding energy.

ionization energies of molecules. On the other hand, 6-31+G(d) is a moderate-size basis set which has enough polarization and diffuse function to reasonably describe the outer valence region of molecule. The blue trace in Figure 11 shows the experimental spectrum which has been shifted about −2.17 eV to match the first feature of the experimental spectrum with the corresponding theoretical spectrum. As seen, there is considerable difference between the experimental and theoretical spectra, especially in the intensities of features. It seems that there is a significant unwanted intensity in the experimental spectrum in the considered energy region compared to the calculated spectrum. Based on these observations (especially, the energy difference between the position of the first feature of the experimental and the calculated spectrum), it can be thought that the β-carotene has been decomposed or degraded at the temperature of the experiment performed by Dougherty et al. (300 °C).[6] For this purpose, the following answer is given here as the reason for this lack of consistency between theory and experiment.

To the best of the present authors' knowledge, there is no report on the thermal stability of β-carotene at 300 °C in the literature. The only report is related to Lemmens et al.'s work, in which effect of thermal processing on the stability of β-carotene was investigated in a broad temperature range (80–150 °C).[72] Based on their experiment, heat induces changes in stability of β-carotene resulting in the conversion of trans isomers to cis isomers in the considered temperature range. Figure 12 demonstrates the photoelectron spectra of some

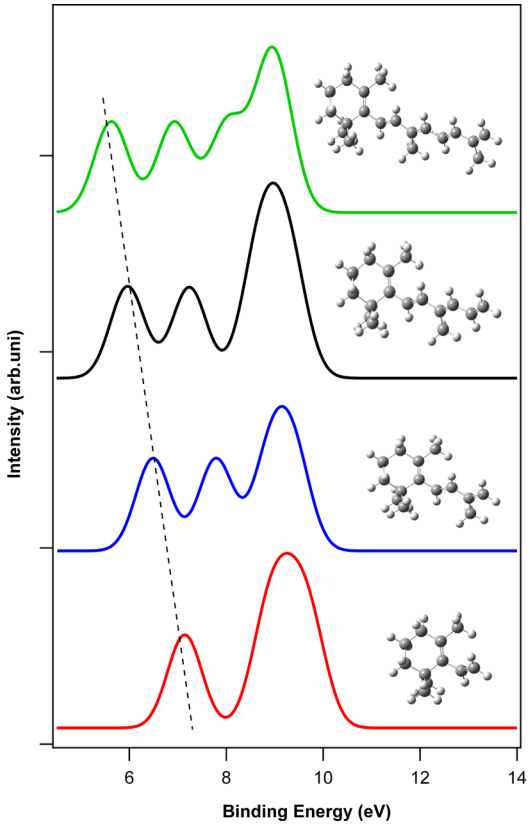

Figure 12. Photoelectron spectra of the selected molecules, shown in the figure, calculated at the SAC-CI SD-R level of theory using the 6-31+G(d) basis set, which may be produced from the fragmentation of β-carotene.

molecules which can be thought to be produced from the fragmentation of β-carotene. The difference among these molecules is related to the length of the polyene chain. It can be seen that, by decreasing length of the polyene chain, the position of the first feature moves to the higher binding energy. In addition, Rademacher et al.[73] recorded the valence photoelectron spectra of some substituted polyene chains with different lengths. They showed that, with the decrease the length of chain, the first feature in the photoelectron spectrum moves to the higher binding energy. This observation can propose that the β-carotene may be decomposed in the

dx.doi.org/10.1021/jp311213c | J. Phys. Chem. B XXXX, XXX, XXX–XXX

experiment of Dougherty et al. because the first feature in their spectrum appeared at 7.65 eV.

4. THEORETICAL CORRELATION BETWEEN THE FIRST IONIZATION ENERGY AND HÜCKEL *K*-INDEX

In this section, the calculated first vertical ionization energies of the considered biological molecules were correlated with their Hückel *k*-indexes. The first ionization energy can be expressed as $I = \alpha + k\beta$, where I is ionization energy, α is Coulomb integral, β is resonance integral, and k is an index. Figure 13a

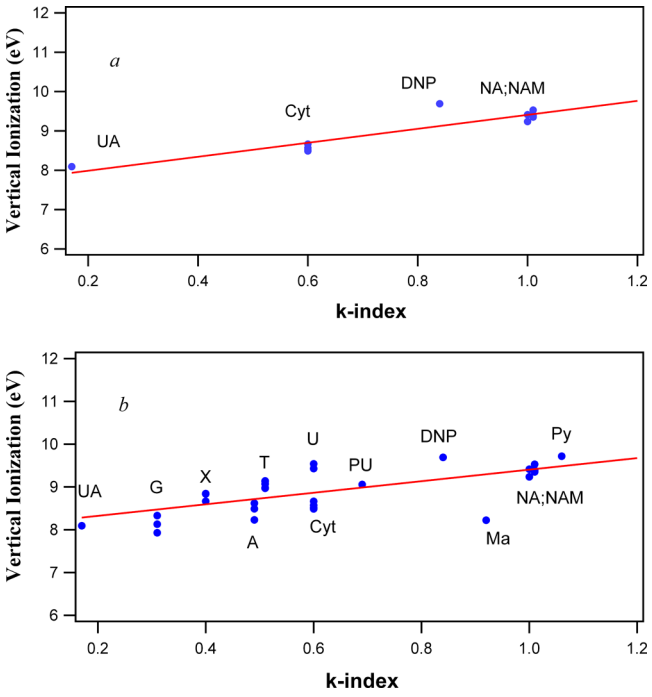

Figure 13. (a) Plot of the first vertical ionization energies, calculated in this work, versus Hückel *k*-index for the selected biochemicals including UA, Cyt, DNP, NA, and NAM. The solid line obeying 7.632 + 1.775*k* is the best least-squares regression line. (b) Similar to (a) but with more selected biochemicals. The solid line obeying 8.0531 + 1.350*k* is the best least-squares regression line.

shows variation of the first vertical ionization energies of DNP, NA, NAM, UA, and Cyt, as calculated in this work, versus their Hückel *k*-indexes. It can be seen that variation of the ionization energies versus *k*-index is almost linear for these molecules. It can be concluded that the energy order of the HOMOs for these molecules is mostly determined based on the values of their *k*-indexes and is independent from the values of α and β. The calculated ionization energies, shown in Figure 13a, were fitted to the $I = \alpha + k\beta$ equation to obtain the values of α and β for these compounds. The values of α and β obtained from the fitting were 7.632 and 1.775 eV, respectively.

To evaluate validation of this correlation, the first ionization energies of a series of heteroatomic biological molecules with known *k*-indexes were predicted using the obtained correlation equation and compared with the corresponding theoretical values reported in the literature (Table 2). The first ionization energy of adenine (A), guanine (G), thymine (T), uracil (U), hypoxanthine (HY), xanthine (X), and menadione (Ma) was predicted using the obtained correlation equation. As seen, there is a good agreement between the predicted ionization energies and those calculated using different theoretical levels

Table 2. Predicted First Vertical Ionization Energies of the Selected Biological Molecules Using Two Selected Correlation Equations Obtained in This Work

		first ionization energy (eV)	
compound	*k*-index	7.632 + 1.775*k*	8.0531 + 1.350*k*
thymine	0.51	8.53	8.74
		(8.97)[a]	
		(9.14)[b]	
		(8.98)[c]	
		(9.07)[d]	
		(9.13)[e]	
adenine	0.49	8.50	8.71
		(8.23)[c]	
		(8.62)[d]	
		(8.49)[e]	
uracil	0.60	8.697	8.86
		(9.43)[d]	
		(9.54)[e]	
guanine	0.31	8.182	8.47
		(7.93)[c]	
		(8.33)[d]	
		(8.13)[e]	
hypoxanthine	0.4	8.342	8.59
		8.845 (tautomer I)[f]	
		8.666 (tautomer II)[f]	
xanthine	0.4	8.342	8.59
		8.839 (tautomer I)[f]	
		8.838 (tautomer II)[f]	
menadione	0.92	9.265	9.29
		9.223[g]	
pyrimidine	1.06	9.513	9.48
		9.719[g]	
purine	0.69	8.856	8.98
		9.057[g]	

[a]EOM-IP-CCSD/CC-pVTZ (ref 15). [b]EOM-IP-CCSD/6-31+G(d) (ref 15). [c]CCSD(T)/aug-cc-pVDZ (ref 16). [d]PMP2/6-31++G(d,p) (ref 74). [e]OVGF-MP2/6-311G(d,p) (ref 75). [f]Direct SAC-CI SD-R/D95+(d,p) (ref 76). [g]The present work.

and basis sets which have been reported in the literature. To obtain a more accurate correlation equation, the theoretical first ionization energies of A, G, T, U, HY, X, and Ma taken from literature and reported in Table 2 as well as the corresponding values calculated in this work were added to the previous points and the linear fitting was repeated (Figure 13b). The predicted first vertical ionization energies which were obtained using the second correlation equation are presented in the fourth column of Table 2.

5. CONCLUSION

The first five ionization energies of some important biomolecules including DNP, DNAN, NA, NAME, NAM, DNAM, BA, Cyt, UA, and β-carotene were calculated using the SAC-CI general-R level of theory. The calculated ionization energies along with their intensities were used to obtain a part of the valence photoelectron spectrum of each molecule. The calculated photoelectron spectrum of each molecule was compared with its experimental spectra reported in the literature. In most cases there was good agreement between the theory and experiment, except for β-carotene. The reason for this disagreement between the calculated and experimental spectrum of β-carotene was attributed to the decomposition of

dx.doi.org/10.1021/jp311213c | J. Phys. Chem. B XXXX, XXX, XXX−XXX

β-carotene due to the relatively high temperature selected by Dougherty et al. (300 °C)[6] for evaporating the sample.

SAC-CI calculations using NBO calculations were also used for assignment of the photoelectron spectra of these molecules. It was found that the primary contribution in the photoelectron lines of the outer valence regions for the considered molecules was due to one-electron processes. As was seen in previous sections, there was an energy shift between the calculated and experimental photoelectron spectrum of each molecule which is also observed in other theoretical levels of theory such as ADC(3) and OVGF methods. The reason for this energy difference can be attributed to the size and incompleteness of the basis set used in the SAC-CI calculations, the basis set and theoretical level which are used for the geometry optimization of molecules and the intrinsic error which is present in the SAC-CI calculations. However, it was demonstrated that the SAC-CI general-R method in combination with the 6-31+G(d) basis set can quite accurately predict the relative energies and intensities of the photoelectron lines of the biological compounds considered in this work.

■ ASSOCIATED CONTENT

Supporting Information

Comparison of the ionization energies of aniline molecule, calculated by the SAC-CI general-R method using 6-31+G(d) basis set, with the corresponding experimental values is shown in Table S1. The calculated main electronic configurations of each ionization band, obtained from the SAC-CI general-R calculations using 6-31+G(d) basis set, along with the dominant natural bonding orbital contributions in the ionized molecular orbitals of the 2,4-dinitrophenol (DNP), 2,4-dinitroanisole (DNAN), conformers of nicotinic acid (NA_1 and NA_2), nicotinic acid methyl ester (NAME), conformers of nicotinamide (NAM_1 and NAM_2), conformers of *N,N*-diethylnicotinamide ($DNAM_1$ and $DNAM_2$), barbituric acid (BA), two tautomers of cytosine (Cyt1 and Cyt2) and uric acid (UA) are shown in Tables S2, S3, S4, S5, S6, S7, S8, S9, S10, S11, S12, S13, and S14, respectively. A sample Gaussian input file of nictotinamide. This material is available free of charge via the Internet at http://pubs.acs.org.

■ AUTHOR INFORMATION

Corresponding Author

*E-mail: farrokhphossein@gmail.com; h-farrokh@cc.iut.ac.ir. Tel.: +98 311 3912343. Fax: +98 311 3912350.

Notes

The authors declare no competing financial interest.

■ ACKNOWLEDGMENTS

The authors are grateful to Isfahan University of Technology (IUT) for its financial support.

■ REFERENCES

(1) Hollas, J. M. *Modern Spectroscopy*; John Wiley & Sons: New York, 1997.

(2) Šponer, J. E.; Sychrovský, V.; Hobza, P.; Šponer, J. Interactions of Hydrated Divalent Metal Cations with Nucleic Acid Bases. How to Relate the Gas Phase Data to Solution Situation and Binding Selectivity in Nucleic Acids. *Phys. Chem. Chem. Phys.* **2004**, *6*, 2772−2780.

(3) Segala, M.; Takahata, Y.; Chong, D. P. Geometry, Solvent, and Polar Effects on the Relationship Between Calculated Core-Electron Binding Energy Shifts (Delta CEBE) and Hammett Substituent (sigma) Constants. *J. Mol. Struct. (THEOCHEM)* **2006**, *758*, 61−69.

(4) Saha, S.; Wang, F.; MacNaughton, J. B.; Moewes, A.; Chong, D. P. The Attachment of Amino Fragment to Purine: Inner-Shell Structures and Spectra. *J. Synchrotron Radiat.* **2008**, *15*, 151−157.

(5) Wang, F.; Downton, T.; Kidwani, N. Adenine Tautomer Electronic Structural Signature Studied Using Dual Space Analysis. *J. Theor. Comput. Chem.* **2005**, *4*, 247−264.

(6) Dougherty, D.; Younathan, E. S.; Voll, R.; Abdulnur, S.; McGlynn, S. P. Photoelectron Spectroscopy of Some Biological Molecules. *J. Electron Spectrosc. Relat. Phenom.* **1978**, *13*, 379−393.

(7) Dougherty, D.; McGlynn, S. P. Photoelectron Spectroscopy of Carbonyls. Biological Molecules. *J. Chem. Phys.* **1977**, *67*, 1289−1290.

(8) Klasinc, L. Application of Photoelectron Spectroscopy to Biologically Active Molecules and Their Constituent Parts. V. Amino Acid Methyl Esters. *Int. J. Quantum Chem.* **1978**, *14*, 373−380.

(9) Klasinc, L.; Novak, I.; Sabljić, A.; McGlynn, S. P. Photoelectron Spectroscopy of Biologically Active Molecules. XVI. Benzophenone Derivatives. *Int. J. Quantum Chem.* **1988**, *34*, 259−266.

(10) Klasinc, L.; RuŠČiĆ, B.; Bhacca, N. S.; Mcglynn, S. P. Application of Photoelectron Spectroscopy to Biologically Active Molecules and Their Constituent Parts XI: Steroids. *Int. J. Quantum Chem.* **1985**, *28*, 161−167.

(11) Klasinc, L.; Mcglynn, S. P.; Paša-Tolić, L. J.; Kovač, B. Photoelectron Spectroscopy of Biologically Active Molecules. 17. Unsaturated Steroids. *Int. J. Quantum Chem.* **1989**, *36*, 331−341.

(12) Paša Tolić, L. J.; Kovač, B.; Klasinc, L.; Shevchenko, S. M.; McGlynn, S. P. Photoelectron Spectroscopy of Biologically Active Molecules. 20. *Para*-quinones, Semiquinones, and Aromatic Ketones. *Int. J. Quantum Chem.* **1990**, *38*, 799−811.

(13) Klasinc, L.; Trinajstića, N.; Knop, J. V. Application of Photoelectron Spectroscopy to Biologically Active Molecules and Their Constituent parts. VIII. Thalidomide. *Int. J. Quantum Chem.* **1980**, *18*, 403−409.

(14) Klasinc, L.; McGlynn, S. P. Photoelectron Spectroscopy of Biologically Active molecules. 21. Thiooxamides. *Int. J. Quantum Chem.* **1990**, *38*, 813−820.

(15) Ghosh, D.; Isayev, O.; Slipchenko, V. L.; Krylov, A. I. Effect of Solvation on the Vertical Ionization Energy of Thymine: From Microhydration to Bulk. *J. Phys. Chem. A* **2011**, *115*, 6028−6038.

(16) Cauet, E.; Valiev, M.; Weare, J. H. Vertical Ionization Potentials of Nucleobases in a Fully Solvated DNA Environment. *J. Phys. Chem. A* **2010**, *114*, 5886−5894.

(17) Farrokhpour, H.; Fathi, F. Naves de Brito, A. Theoretical and Experimental Study of Valence Photoelectron Spectrum of D,L-Alanine Amino Acid. *J. Phys. Chem. A* **2012**, *116*, 7004−7015.

(18) Jagoda-Cwiklik, B.; Slavicek, P.; Cwiklik, L.; Nolting, D.; Winter, B.; Jungwirth, P. Emergence of Charge-Transfer-to-Solvent Band in the Absorption Spectra of Hydrogen Halides on Ice Nanoparticles: Spectroscopic Evidence for Acidic Dissociation. *J. Phys. Chem. A* **2008**, *112*, 3499−3505.

(19) Vonderach, M.; Ehrler, O. T.; Matheis, K.; Weis, P.; Kappes, M. M. Isomer-Selected Photoelectron Spectroscopy of Isolated DNA Oligonucleotides: Phosphate and Nucleobase Deprotonation at High Negative Charge States. *J. Am. Chem. Soc.* **2012**, *134*, 7830−7841.

(20) Feyer, V.; Plekan, O.; Richter, R.; Coreno, M.; Prince, K. C.; Carravetta, V. Core Level Study of Alanine and Threonine. *J. Phys. Chem. A* **2008**, *112*, 7806−7815.

(21) Plekan, O.; Feyer, V.; Richter, R.; Coreno, M.; De Simone, M.; Prince, K. C.; Trofimov, A. B.; Gromov, E. V.; Zaytseva, I. L.; Schirmer, J. A Theoretical and Experimental Study of the Near Edge X-ray Absorption Fine Structure (NEXAFS) and X-ray Photoelectron Spectra (XPS) of Nucleobases: Thymine and Adenine. *Chem. Phys.* **2008**, *347*, 360−375.

(22) Plekan, O.; Feyer, V.; Richter, R.; Coreno, M.; Vall-llosera, G.; Prince, K. C.; de Simone, M.; Trofimov, A. B.; Zaytseva, I. L.; Moskovskaya, T. E.; et al. An Experimental and Theoretical Core-Level Study of Tautomerism in Guanine. *J. Phys. Chem. A* **2009**, *113*, 9376−9385.

(23) Zaytseva, I. L.; Trofimov, A. B.; Schirmer, J.; Plekan, O.; Feyer, V.; Richter, R.; Coreno, M.; Prince, K. C. Theoretical and Experimental Study of Valence-Shell Ionization Spectra of Guanine. *J. Phys. Chem. A* **2009**, *113*, 15142−15149.
(24) Feyer, V.; Plekan, O.; Richter, R.; Coreno, M.; Prince, K. C.; Carravetta, V. Photoemission and Photoabsorption Spectroscopy of Glycyl-Glycine in the Gas Phase. *J. Phys. Chem. A* **2009**, *113*, 10726−10733.
(25) Powis, I.; Rennie, E. E.; Hergenhahn, U.; Kugeler, O.; Bussy-Socrate, R. Investigation of the Gas-Phase Amino Acid Alanine by Synchrotron Radiation Photoelectron Spectroscopy. *J. Phys. Chem. A* **2003**, *107*, 25−34.
(26) Feyer, V.; Plekan, O.; Richter, R.; Coreno, M.; Vall-llosera, G.; Prince, K. C.; Trofimov, A. B.; Zaytseva, I. L.; Moskovskaya, T. E.; Gromov, E. V.; et al. Tautomerism in Cytosine and Uracil: An Experimental and Theoretical Core Level Spectroscopic Study. *J. Phys. Chem. A* **2009**, *113*, 5736−5742.
(27) Nakatsuji, H. Description of Two- and Many-Electron Processes by the SAC-CI method. *Chem. Phys. Lett.* **1991**, *177*, 331−337.
(28) Nakatsuji, H. Multireference Cluster Expansion Theory: MR−SAC Theory. *J. Chem. Phys.* **1985**, *83*, 713−722.
(29) Nakatsuji, H. Exponentially Generated Wave Functions. *J. Chem. Phys.* **1985**, *83*, 5743−5748.
(30) Nakatsuji, H. Exponentially Generated Configuration Interaction Theory. Descriptions of Excited, Ionized, and Electron Attached States. *J. Chem. Phys.* **1991**, *94*, 6716−6727.
(31) Nakatsuji, H.; Kitao, O.; Yonezawa, T. Cluster Expansion of the Wave Function. Valence and Rydberg Excitations and Ionizations of Pyrrole, Furan, and Cyclopentadiene. *J. Chem. Phys.* **1985**, *83*, 723−734.
(32) Nakatsuji, H.; Saito, S. Calculation of Hyperfine Splitting Constants with Slater-Type Cusp Basis by the Symmetry Adapted Cluster-Configuration Interaction theory. *J. Chem. Phys.* **1989**, *91*, 6205−6214.
(33) Nakatsuji, H.; Ehara, M.; Palmer, M. H.; Guest, M. F. Theoretical Study on the Excited and Ionized States of Titanium Tetrachloride. *J. Chem. Phys.* **1992**, *97*, 2561−2570.
(34) Nakatsuji, H.; Ehara, M. Symmetry Adapted Cluster-Configuration Interaction Study on the Excited and Ionized. *J. Chem. Phys.* **1994**, *101*, 7658−7671.
(35) Nakatsuji, H.; Hasegawa, J.; Hada, M. Excited and Ionized States of Free Base Porphin Studied by the Symmetry Adapted Cluster-Configuration Interaction (SAC-CI) method. *J. Chem. Phys.* **1996**, *104*, 2321−2330.
(36) Ehara, M.; Ohtsuka, Y.; Nakatsuji, H. Ionization Spectra of $XONO_2$ (X=F, Cl, Br, I) Studied by the SAC-CI Method. *Chem. Phys.* **1998**, *226*, 113−123.
(37) Ehara, M.; Nakatsuji, H. Ionization Spectrum of CO_2 Studied by the SAC-CI General-*R* Method. *Spectrochim. Acta, Part A* **1999**, *55*, 487−493.
(38) Ehara, M.; Nakatsuji, H. Outer- and Inner-Valence Ionization Spectra of N_2 and CO:: SAC-CI (General-R) Compared with Full-CI Spectra. *Chem. Phys. Lett.* **1998**, *282*, 347−354.
(39) Hasegawa, J.; Ehara, M.; Nakatsuji, H. Theoretical Study on the Ionized States of Ethylene by the SAC-CI (General-*R*) Method. *Chem. Phys.* **1998**, *230*, 23−30.
(40) www.qcri.or.jp/sacci/.
(41) Martin, R. I.; Shirley, D. A. Theory of Core-Level Photoemission Correlation State Spectra. *J. Chem. Phys.* **1976**, *64*, 3685−3690.
(42) Glendening, E. D.; Carpenter, A. E.; Reed, A. E.; Weinhold, F. *NBO Version 3.1*; University of Wisconsin: Madison, WI, 1995.
(43) Frisch, M. J.; Trucks, G. W.; Schlegel, H. B.; Scuseria, G. E.; Robb, M. A.; Cheeseman, J. R.; Scalmani, G.; Barone, V.; Mennucci, B.; Petersson, G. A.; Nakatsuji, H.; Caricato, M.; Li, X.; Hratchian, H. P.; Izmaylov, A. F.; Bloino, J.; Zheng, G.; Sonnenberg, J. L.; Hada, M.; Ehara, M.; Toyota, K.; Fukuda, R.; Hasegawa, J.; Ishida, M.; Nakajima, T.; Honda, Y.; Kitao, O.; Nakai, H.; Vreven, T.; Montgomery, J. A., Jr.; Peralta, J. E.; Ogliaro, F.; Bearpark, M.; Heyd, J. J.; Brothers, E.; Kudin, K. N.; Staroverov, V. N.; Kobayashi, R.; Normand, J.; Raghavachari, K.; Rendell, A.; Burant, J. C.; Iyengar, S. S.; Tomasi, J.; Cossi, M.; Rega, N.; Millam, J. M.; Klene, M.; Knox, J. E.; Cross, J. B.; Bakken, V.; Adamo, C.; Jaramillo, J.; Gomperts, R.; Stratmann, R. E.; Yazyev, O.; Austin, A. J.; Cammi, R.; Pomelli, C.; Ochterski, J. W.; Martin, R. L.; Morokuma, K.; Zakrzewski, V. G.; Voth, G. A.; Salvador, P.; Dannenberg, J. J.; Dapprich, S.; Daniels, A. D.; Farkas, O.; Foresman, J. B.; Ortiz, J. V.; Cioslowski, J.; Fox, D. J. *Gaussian 09, Revision B.01*; Gaussian, Inc.: Wallingford, CT, 2009.
(44) Kimura, K.; Katsumata, S.; Achiba, Y.; Yamazaki, T.; Iwata, S. *Handbook of HeI Photoelectron Spectra of Fundamental Organic Molecules*; Japan Scientific Societies: Tokyo, 1981; p 190.
(45) Genoni, G. P.; Behra, R.; Montague, C. L.; Güttinger, H.; Ternay-Aegerter, R. Complex Dynamics of Adaptation in a Nonaxenic Microcystis Culture: 1. Effects of Dinitrophenol on Population Growth. *Ecotoxicol. Environ. Safety* **2001**, *48*, 235−240.
(46) Chudgar, J.; Oakes, J. *Kirk-Othmer Encyclopedia of Chemical Technology—Section on Azo Dyes*; John Wiley & Sons, Inc.: New York, 2003.
(47) Koopmans, T. Über die Zuordnung von Wellenfunktionen und Eigenwerten zu den Einzelnen Elektronen Eines Atoms. *Physica* **1934**, *1*, 104−113.
(48) LaFemina, J. P. Ultraviolet Photoelectron and Absorption Spectra of Substituted Phenols. *Int. J. Quantum Chem.* **1989**, *36*, 563−573.
(49) Palmer, M. H.; Moyes, W.; Speirs, M. The Electronic Structure of Substituted Benzenes; ab Initio Calculations and Photoelectron Spectra for Phenol, the Methyl- and Fluoro-Derivatives, and the Dihydroxybenzenes. *J. Mol. Struct.* **1979**, *52*, 293−307.
(50) Rabalais, J. W. Photoelectron Spectroscopic Investigation of the Electronic Structure of Nitromethane and Nitrobenzene. *J. Chem. Phys.* **1972**, *57*, 960−968.
(51) Blum, R. *Ullmann's Encyclopedia of Industria Chemistry-section on Vitamins*; Wiley-VCH Verlag GmbH & Co.: Weinheim, Germany, 2002.
(52) Caselli, A.; Hanane, T.; Jane, B.; Carter, S.; Khaodhiar, L.; Veves, A. J. Topical Methyl Nicotinate-Induced Skin Vasodilation in Diabetic NeuropathyDiabetes and Its Complications. *J. Diabetes Complications* **2003**, *17*, 205−210.
(53) Opitz, J. Electron-Impact Ionization of Benzoic Acid, Nicotinic Acid and their *n*-Butyl Esters: An Approach to Regioselective Proton Affinities Derived from Ionization and Appearance Energy Data. *Int. J. Mass. Spectrom.* **2007**, *265*, 1−14.
(54) Stefanović, D.; Grützmacher, H. F. The Ionization Potential of some Substituted Pyridines. *Org. Mass Spectrom.* **1974**, *9*, 1052−1054.
(55) Kamat, J. P.; Devasagayam, T. P. Nicotinamide (vitamin B3) as an Effective Antioxidant Against Oxidative Damage in Rat Brain Mitochondria. *Redox Rep.* **1999**, *4*, 179−184.
(56) Pero, R. W.; Axelasson, B.; Riemann, D. Newly Discovered Anti-Inflammatory Properties of the Benzamides and Nicotinamides. *Mol. Cell. Biochem.* **1999**, *193*, 119−125.
(57) Zhou, W. J.; Kurth, M. J. Synthesis of a Novel pH-Responding Polymer with Pendant Barbituric Acid Moieties. *Polymer* **2001**, *42*, 345−349.
(58) Thetford, D.; Chorlton, A. P.; Hardman, J. Synthesis and Properties of some Polycyclic Barbiturate Pigments. *Dyes Pigm.* **2003**, *59*, 185−191.
(59) Boylan, J. C.; Swarbrick, J. *Encyclopedia of Pharmaceutical Technology*; Dekker: New York, 2002.
(60) Ralhan, S.; Ray, N. K. Density Functional Study of Barbituric Acid and Its Tautomers. *J. Mol.. Struct. (Theochem)* **2003**, *634*, 83−88.
(61) Chahwan, R.; Wontakal, S. N.; Roa, S. Crosstalk Between Genetic and Epigenetic Information Through Cytosine Deamination. *Trends Genet.* **2010**, *26*, 443−448.
(62) Yu, C.; Peng, S.; Akiyama, I.; Lin, J.; Le Breton, P. R. Ultraviolet Photoelectron Studies of Biological Pyrimidines. The valence electronic structure of cytosine. *J. Am. Chem. Soc.* **1978**, *100*, 2303−2307.

(63) Trofimov, A. B.; Schirmer, J.; Kobychev, V. B.; Potts, A. W. ; Holland, D. M. P.; Karlsson, L. *J. Phys. B: At.* Photoelectron Spectra of the Nucleobases Cytosine, Thymine and Adenine. *Mol. Opt. Phys.* **2006**, *39*, 305-329.
(64) Dolgounitcheva, O.; Zakrzewski, V. G.; Ortiz, J. V. Ionization Energies and Dyson Orbitals of Cytosine and 1-Methylcytosine. *J. Phys. Chem. A.* **2003**, *107*, 822−828.
(65) Fogarasi, G. Relative Stabilities of Three Low-Energy Tautomers of Cytosine: A Coupled Cluster Electron Correlation Study. *J. Phys. Chem. A* **2002**, *106*, 1381−1390.
(66) Guan, Y.; Chu, Q.; Ye, J. Determination of Uric Acid in Human Saliva by Capillary Electrophoresis with Electrochemical Detection: Potential Application in Fast Diagnosis of Gout. *Anal. Bioanal. Chem.* **2004**, *380*, 913−917.
(67) Hayden, M. R.; Tyagi, S. C. Uric Acid: A New Look at an Old Risk Marker for Cardiovascular Disease, Metabolic Syndrome, and type 2 diabetes mellitus: The Urate Redox Shuttle. *Nutr. Metabolism* **2004**, *1*, 10.
(68) Ames, B. N.; Cathcart, R.; Schwiers, E.; Hochstein, P. Uric Acid Provides an Antioxidant Defense in Humans Against Oxidant- and Radical-Caused Aging and Cancer: a Hypothesis. *Proc. Natl. Acad. Sci.* **1981**, *78*, 6858−6862.
(69) El-Agamey, A.; Lowe, G.; McGarvey, D.; Mortensen, A.; Phillip, D.; Truscott, T.; Young, A. Carotenoid Radical Chemistry and Antioxidant/Pro-oxidant Properties. *Arch. Biochem. Biophys.* **2004**, *430*, 37−48.
(70) Gao, Y.; Kispert, L. D.; Konovalova, T. A.; Lawrence, J. N. Isomerization of Carotenoids in the Presence of MCM-41 Molecular Sieves: EPR and HPLC Studies. *J. Phys. Chem. B.* **2004**, *108*, 9456−828.
(71) Ceron-Carrasco, J. P.; Bastida, A.; Zuniga, J.; Requena, A.; Miguel, A. Density Functional Theory Study of the Stability and Vibrational Spectra of the β-Carotene Isomers. *J. Phys. Chem. A* **2009**, *113*, 9899−9907.
(72) Lemmens, L.; De Vleeschouwer, K.; Moelants; Katlijn, R. N.; Colle, Ines, J. P.; Loey, Van.; Hendrickx; Marc, E. J. β-Carotene Isomerization Kinetics During Thermal Treatments of Carrot Puree. *J. Agric. Food. Chem.* **2010**, *58*, 6816−6824.
(73) Radermacher, P.; Kowski, K.; Hopf, H.; Klein, D.; Klein, O.; Suhrada, C. Photoelectron Spectra and Electronic Structures of Highly Substituted Polyenes. *J. Mol. Struct.* **2001**, *567−568*, 11−18.
(74) Crespo-Hernandez, C. E.; Arce, R.; Ishikawa, Y.; Gorb, L.; Leszcynski, J. Close, David M. Ab Initio Ionization Energy Thresholds of DNA and RNA Bases in Gas Phase and in Aqueous Solution. *J. Phys. Chem. A* **2004**, *108*, 6373−6377.
(75) Close, D. M. Calculation of the Ionization Potentials of the DNA Bases in Aqueous Medium. *J. Phys. Chem. A* **2004**, *108*, 10376−10379.
(76) Farrokhpour, H.; Fathi, F. Theoretical Study of Valance Photoelectron Spectra of Hypoxanthine, Xanthine, and Caffeine Using Direct Symmetry-Adapted Cluster/Configuration Interaction Methodology. *J. Comput. Chem.* **2011**, *32*, 2479−2491.